

Design of a Multiband Frequency Selective Surface

Dong Ho Kim and Jae Ick Choi

ABSTRACT—A frequency selective surface (FSS), whose unit cell consists of a ternary tree loop loaded with a modified tripole, is proposed to block multiple frequency bands. Target frequency bands correspond to Korean personal communication services, cellular mobile communication, and 2.4 GHz industrial, scientific, and medical bands. Through the adjustment of inter-element and inter-unit cell gaps, and adjustment of the length of elements, we present an FSS design method that makes the precise tuning of multiple resonance frequencies possible. Additionally, to verify the validity of our approach, simulation results obtained from a commercial software tool and experimental data are also presented.

Keywords—Frequency selective surface (FSS), tripole, ternary tree loop, unit cell, equivalent capacitance.

I. Introduction

There are many application areas adopting frequency selective surfaces (FSSs) such as antenna radomes, dichroic reflectors, artificial magnetic conductors, waveguide applications, and so on [1]–[3]. To meet the requirements of those application purposes, many things should be considered at the design stage of FSSs; selection of the appropriate unit-cell geometry, electrical properties of dielectric material, thickness of the FSSs, spacing between unit cells, and so on [4].

There have been several approaches to obtaining multiple resonance properties, which include consisting of a unit cell with geometrically the same shape but different sized elements [3], [4] or with fractal geometry [5], [6].

In this letter, we focus on a multiband blocking application through the design of a unit cell consisting of a ternary tree shaped loop loaded with a tripole. The resonance behavior of an FSS composed of a single ternary tree loop or a single tripole is relatively well understood [7], [8]. However, to our

knowledge, an FSS with a unit cell made up of those two elements together has not been treated carefully. Therefore, we propose a ternary tree loop combined with a tripole as our unit cell geometry. Additionally, we present a successfully frequency-tuned response of our FSS by considering the effect of the equivalent capacitance between unit cell elements. To confirm the validity of our approach, experimental data are presented with the simulation results achieved by CST Microwave Studio (MWS) and Ansoft HFSS.

II. FSS Design and Measurement Results

The proposed unit cell geometry of our FSS is depicted in Fig. 1. Our FSS unit cell consists of two modified conducting elements: a ternary tree shaped loop and a tripole loaded inside the loop. To increase the equivalent capacitance between elements, each end part of the element is shaped to fit exactly with the adjacent element as shown in Fig. 1.

The unit cell elements are made up of copper etched on a thin 80 cm × 80 cm polyethylene terephthalate resin (PET) film of $\epsilon_r = 3.3$ and $\mu_r = 1.0$ to minimize the effect of the dielectric material. The thicknesses of the copper and substrate PET film are 35.0 μm and 76.2 μm , respectively. A fabricated unit cell array of our FSS is shown in Fig. 1(b).

Using the well-known circuit theory, our FSS can be equivalently interpreted as a resonant circuit consisting of parallel-connected two series L-C resonators as shown in Fig. 2. In Fig. 2, L_1 and L_2 denote equivalent inductances of a tripole and a ternary tree loop, respectively, and C_1 and C_2 indicate that the equivalent capacitances correspond to the inter-element gap in the same unit cell and the inter-unit cell gap between the adjacent unit cells, respectively. It is important to note that those capacitances are basically affected by the permittivity of the substrate material. We do not consider the higher resonance mode of the loop in our equivalent circuit representation, which occurs near 2.6 GHz in Fig. 3.

Manuscript received Nov. 24, 2005; revised June 13, 2006.

Dong Ho Kim (phone: + 82 42 860 6575, email: dhkim@etri.re.kr) and Jae Ick Choi (email: jichoi@etri.re.kr) are with Digital Broadcasting Research Division, ETRI, Daejeon, Korea.

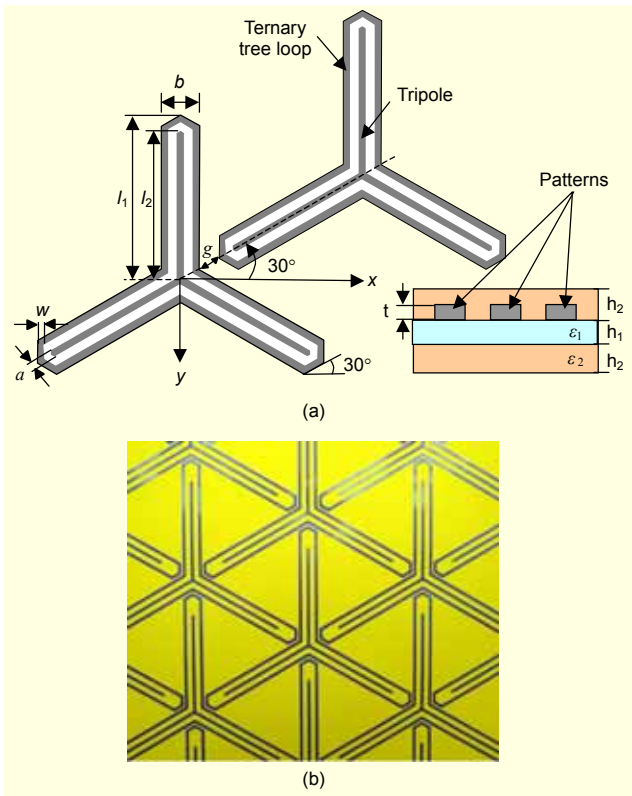


Fig. 1. (a) Geometry and parameters of a unit cell, and (b) fabricated unit cell array on a PET film.

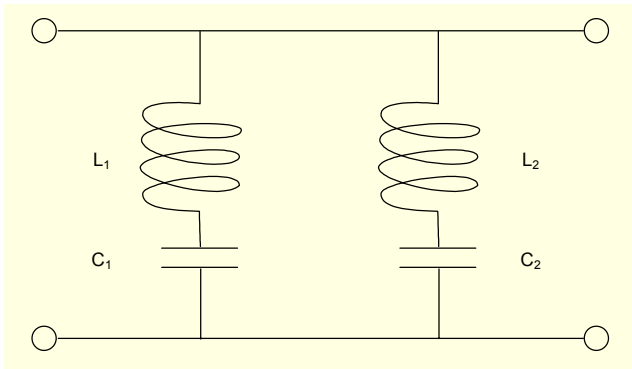


Fig. 2. Equivalent circuit representation of our structure.

Tuning of the resonance frequencies of our FSS can be described in two steps. The first is determining the total length of elements to make the FSS resonate at somewhat higher frequencies than the target frequencies. The second is adjusting the gaps equivalently represented as the two capacitors in Fig. 2. In the first step, because the first resonance frequencies of the FSS are mainly determined by the circumferential length of elements, there may be no large ‘degree-of-freedom’ in control of the inter-element gap, which is represented by C_1 . Consequently, the spacing between adjacent unit cells, which equivalently corresponds to C_2 , can be the more dominant

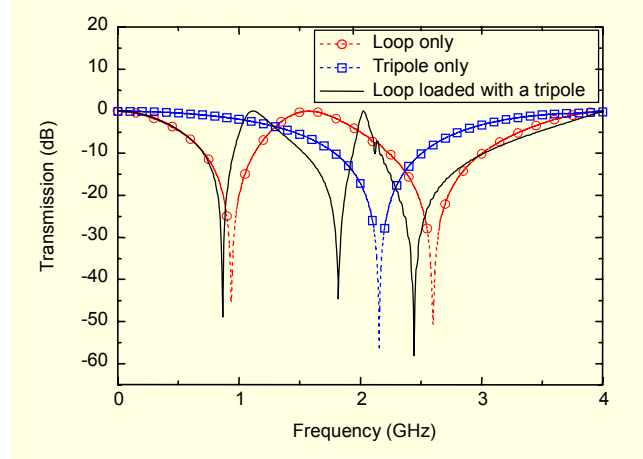


Fig. 3. Resonance frequency response of several unit cells with $a=1.5\text{mm}$, $b=5\text{mm}$, $w=g=1\text{mm}$, $l_1=25.8\text{mm}$, $l_2=21.2\text{mm}$, $t=35\ \mu\text{m}$, $h_1=76.2\ \mu\text{m}$, $h_2=1.6\ \text{mm}$, $\epsilon_1=3.3$, and $\epsilon_2=4.5$.

parameter in fine-tuning of the overall resonance frequencies.

Figure 3 shows the resonant frequency variation due to the loading of an inner tripole under the normal incidence of a horizontally polarized (E_x) plane wave. The red line with circular symbols represents the resonance characteristic of the FSS with unit cells consisting of a ternary tree loop only. The resonances near 0.94 GHz ($=\tilde{f}_1$) and 2.6 GHz ($=\tilde{f}_3$) are due to the first and the second resonances of the loop, respectively. The blue curve with rectangular symbols implies the frequency response of a single tripole, whose resonance is near 2.2 GHz ($=\tilde{f}_2$). The black solid line shows the effect of a tripole loading, and the downward shift of an overall frequency response is remarkable. Table 1 shows the variation of reflecting center frequencies and bandwidths caused by the loading of tripole. The frequency shift ratio of the tripole (f_2 / \tilde{f}_2) is smaller than those of the loop. This is because both capacitors contribute to the downward shift of the resonant frequency of the tripole. It is also worth noting that the bandwidth reduction ratio for the loop’s second resonance (B_3 / \tilde{B}_3) is increased.

Figure 4 shows the variation of resonance frequencies due to the change of inter-unit cell distance, g . Lines with circular and rectangular symbols indicate the first and second resonance frequencies of each element, respectively.

As Fig. 4 indicates, resonance frequencies are the function of the spacing between unit cells. While the first resonance frequencies of both elements increase with respect to the increase of the spacing, the second resonance frequency of the loop decreases. The increase of the first resonance frequencies occurs mainly because the longer inter-unit cell distance results in the smaller capacitance of C_2 . But, the blue line with rectangular symbols represents the higher mode of the loop; therefore, it is inversely proportional to the first resonance behavior.

Table 1. Frequency and bandwidth variations caused by tripole loading.

| Target frequency (MHz) | | | 20 dB bandwidth (MHz) | | | Frequency shift ratio | | | Bandwidth reduction ratio | | |
|------------------------|-------|-------|-----------------------|-------|-------|-----------------------|-------------------|-------------------|---------------------------|-------------------|-------------------|
| f_1 | f_2 | f_3 | B_1 | B_2 | B_3 | f_1/\tilde{f}_1 | f_2/\tilde{f}_2 | f_3/\tilde{f}_3 | B_1/\tilde{B}_1 | B_2/\tilde{B}_2 | B_3/\tilde{B}_3 |
| 859 | 1810 | 2445 | 75 | 130 | 245 | 0.91 | 0.84 | 0.93 | 0.58 | 0.59 | 1.2 |

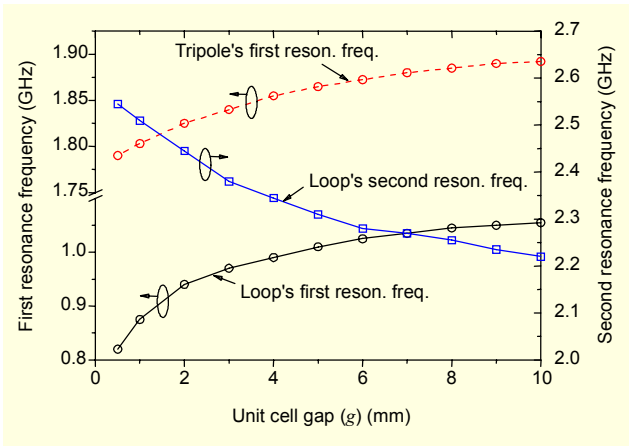


Fig. 4. Resonance frequency variation with respect to the unit cell gap for the same parameters used in Fig. 2.

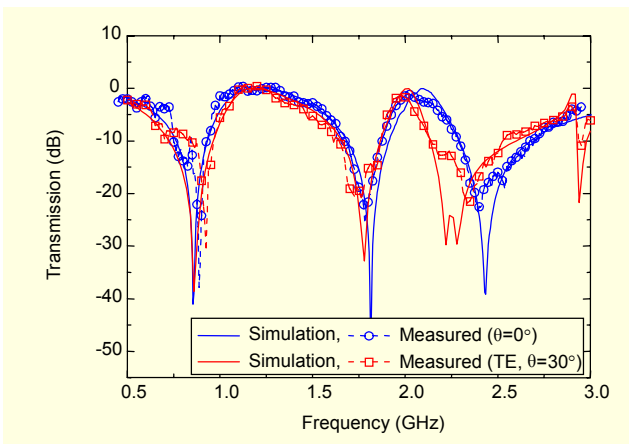


Fig. 5. Predicted and experimental data for $a=1$ mm, $b=7.5$ mm, $w=g=1$ mm, $l_1=472$ mm, $l_2=40.2$ mm, $t=35$ μ m, $h_1=76.2$ μ m, $h_2=0$ mm, and $\epsilon_1=3.3$.

Based on our tuning method and resonance characteristics given in Fig. 4, the predicted and measured transmission losses of our FSS, which is fabricated as shown in Fig. 1(b), are given in Fig. 5. The same target center frequencies given in Table 1 are used. Lines with circular and rectangular symbols indicate the measured data with normal and inclined incidences, respectively. The overall frequency resonance behavior of our FSS shows relatively good agreement with the predicted resonance curve.

III. Conclusion

A frequency selective surface for the blocking of multiple frequency bands has been proposed. We have selected Korean cellular mobile communication (800 MHz band), PCS (1.8 GHz band), and 2.4 GHz ISM bands as target frequency bands. By applying the proposed design and tuning procedure, we can successfully put the center resonant frequencies of our FSS exactly onto the designated target frequencies. For our future work, we are improving our structure to obtain a wider bandwidth and stable angular sensitivity, simultaneously.

References

- [1] J. Huang, T. K. Wu, and S. W. Lee, "Tri-Band Frequency Selective Surface with Circular Ring Elements," *IEEE Trans. Antennas Propagat.*, vol. 42, no.2, Feb. 1994, pp.166-175.
- [2] E. L. Pelton and B. A. Munk, "A Streamlined Metallic Radome," *IEEE Trans. Antennas Propagat.*, vol. 22, no.6, Nov. 1974, pp.799-803.
- [3] T. K. Wu, "Four-Band Frequency Selective Surface with Double-Square-Lop Patch Elements," *IEEE Trans. Antennas Propagat.*, vol. 42, no.12, Dec. 1994, pp.1659-1663.
- [4] J. P. Gianvittorio, J. Romeu, S. Blanch, and Y. Rahmat-Samii, "Self-Similar Prefractal Frequency Selective Surfaces for Multiband and Dual-Polarized Applications," *IEEE Trans. Antennas and Propagat.*, vol. 51, no. 11, Nov. 2003, pp.3088-3096.
- [5] J. Yeo and R. Mittra, "Numerically Efficient Analysis of Microstrip Antennas Using the Characteristic Basis Function Method (CBFM)," *IEEE AP Society Int'l Symp. 2003.*, vol. 4, Jun. 2003, pp.85-88.
- [6] D. H. Werner and D. Lee, "Design of Dual-Polarised Multiband Frequency Selective Surfaces Using Fractal Elements," *Electronics Lett.*, vol. 36, no. 6, Mar. 2000, pp.487-488.
- [7] B. A. Munk, *Frequency Selective Surfaces: Theory and Design*, John Wiley & Sons, Inc., 2000, pp.1-62.
- [8] L. S. Riggs and R. G. Smith, JR., "Efficient Current Expansion Modes for the Triarm Frequency-Selective Surface," *IEEE Trans. Antennas and Propagat.*, vol. 36, no. 8, Aug. 1988, pp.1172-1177.